MOLECULAR AND CELLULAR BIOLOGY, Dec. 2008, p. 7168–7181 Vol. 28, No. 23
0270-7306/08/$08.00+0 doi:10.1128/MCB.00256-08

Dual Roles for NFAT Transcription Factor Genes as Oncogenes and Tumor Suppressors▽†

Bruno K. Robbs,[1,2] Andre L. S. Cruz,[1] Miriam B. F. Werneck,[1]‡ Giuliana P. Mognol,[1] and João P. B. Viola[1]*

Division of Cellular Biology, Brazilian National Cancer Institute (INCA), Rio de Janeiro, Brazil,[1] and Carlos Chagas Filho Biophysics Institute, Federal University of Rio de Janeiro (UFRJ), Rio de Janeiro, Brazil[2]

Received 14 February 2008/Returned for modification 14 April 2008/Accepted 13 September 2008

Nuclear factor of activated T cells (NFAT) was first described as an activation and differentiation transcription factor in lymphocytes. Several in vitro studies suggest that NFAT family members are redundant proteins. However, analysis of mice deficient for NFAT proteins suggested different roles for the NFAT family of transcription factors in the regulation of cell proliferation and apoptosis. NFAT may also regulate several cell cycle and survival factors influencing tumor growth and survival. Here, we demonstrate that two constitutively active forms of NFAT proteins (CA-NFAT1 and CA-NFAT2 short isoform) induce distinct phenotypes in NIH 3T3 cells. Whereas CA-NFAT1 expression induces cell cycle arrest and apoptosis in NIH 3T3 fibroblasts, CA-NFAT2 short isoform leads to increased proliferation capacity and induction of cell transformation. Furthermore, NFAT1-deficient mice showed an increased propensity for chemical carcinogen-induced tumor formation, and CA-NFAT1 expression subverted the transformation of NIH 3T3 cells induced by the H-*rasV12* oncogene. The differential roles for NFAT1 are at least partially due to the protein C-terminal domain. These results suggest that the NFAT1 gene acts as a tumor suppressor gene and the NFAT2 short isoform acts gene as an oncogene, supporting different roles for the two transcription factors in tumor development.

The nuclear factor of activated T cells (NFAT) family of transcription factors, first described as a regulator of T-cell activation, is composed of four calcium-responsive proteins named NFAT1 (NFATc2/NFATp), NFAT2 (NFATc1/NFATc), NFAT3 (NFATc4), and NFAT4 (NFATc3/NFATx). All NFAT proteins share a common DNA-binding domain (DBD) that has a moderate sequence similarity to the DBD of the Rel family of transcription factors. This domain endows all NFAT proteins with the specificity to bind the DNA core sequence A/TGGAAA (38). NFAT proteins also share a regulatory conserved N-terminal region called the NFAT homology region (NHR). This region is highly phosphorylated in resting cells, keeping NFAT in an inactive state and restricted to the cytoplasm. An increase in intracellular calcium activates calcineurin, a calcium/calmodulin-dependent serine/threonine phosphatase that directly dephosphorylates the NHR, allowing NFAT to translocate to the nucleus and increase its DNA affinity (12, 41). Once located in the nucleus, NFAT proteins can bind to their target promoter elements and activate the transcription of specific responsive genes, either alone or in combination with other nuclear partners (25). Each NFAT gene may be alternatively spliced into two or more isoforms that differ at the amino and/or carboxyl termini, although the core of the DBD region remains conserved. Additionally, a transactivation domain located in the variable regions in NFAT has been identified (38).

NFAT1 and NFAT2 are the prevalent NFAT family members expressed in peripheral T lymphocytes. Upon T-cell receptor stimulation, NFAT leads to a change in the expression of a number of cytokine genes, including those for interleukin 2 (IL-2), IL-3, IL-4, IL-5, and gamma interferon. However, NFAT also regulates other responsive genes, like those for $p21^{Waf1}$, CD40 ligand, FasL, CDK4, and cyclin A2, indicating that these transcription factors may also be involved in the control of the cell cycle and apoptosis (7, 42). Although NFAT1 and NFAT2 share 72% sequence similarity in their DBDs and act similarly in functional assays, mice deficient in either of these two genes have markedly divergent phenotypes. Three-month-old $NFAT1^{-/-}$ mice develop a lymphocyte hyperproliferative phenotype that is reflected in a mild size increase in peripheral lymphoid organs accompanied by a reduction in cell death and an increased cell cycle rate (6, 19, 39, 44). $NFAT1^{-/-}$ mice also develop neoplastic transformation of cartilage cells that resemble chondrosarcomas (37). In contrast, $NFAT2^{-/-}$ mice die in utero due to a defect in the development of cardiac valves and septa (13, 35). Interestingly, peripheral $NFAT2^{-/-}$ T cells from chimeric $NFAT2^{-/-} \times RAG^{-/-}$ mice show impaired proliferation with no apparent defect in apoptosis (36, 45).

The phenotypes of NFAT-deficient mice suggest that this family of transcription factors is likely to play a much broader role in the regulation of cell growth and apoptosis than previously described. Furthermore, divergent functions between NFAT1 and NFAT2 proteins in cell transformation may exist but have not yet been characterized. To address these hypoth-

* Corresponding author. Mailing address: Divisão de Biologia Celular, Instituto Nacional de Câncer (INCA), Rua André Cavalcanti, 37, Centro, Rio de Janeiro, RJ, Brazil 20231-050. Phone: (55-21) 3233-1322. Fax: (55-21) 3233-1470. E-mail: jpviola@inca.gov.br.

‡ Present address: Division of Biological Sciences, University of California, San Diego, CA.

† Supplemental material for this article may be found at http://mcb.asm.org/.

▽ Published ahead of print on 22 September 2008.

eses, we utilized previously characterized constitutively active NFAT1 (CA-NFAT1) and NFAT2 short isoform (CA-NFAT2/A) mutants, which are known to be constitutively localized in the nucleus, to bind DNA with high affinity and to activate endogenous NFAT target genes (29, 31). Thus, we used constitutively active proteins to analyze the effects of sustained NFAT activation on the cell cycle and apoptosis. Remarkably, ectopic expression of CA-NFAT1 and CA-NFAT2 short isoform in NIH 3T3 fibroblasts produced opposite phenotypes in the regulation of the cell cycle, apoptosis, and cell transformation. We observed that NFAT2 short isoform acts as a positive regulator of cell proliferation, a repressor of cell death, and an inducer of cell transformation. Conversely, NFAT1 enhanced cell death, repressed the cell cycle, and subverted cell transformation. Taken together, these results strongly suggest that NFAT1 and NFAT2 genes have important, opposing roles in the control of the cell cycle and apoptosis. Furthermore, NFAT1 and NFAT2 short isoform genes may function as a tumor suppressor or an oncogene, respectively, suggesting a putative role in tumor development.

MATERIALS AND METHODS

Animals and cell culture. Athymic BALB/c nude/nude, NFAT1$^{+/+}$, and NFAT1$^{-/-}$ mice were maintained in the Brazilian National Cancer Institute animal facility. NFAT1$^{+/+}$ and NFAT1$^{-/-}$ (C57BL/6 × 129/Sv) mice were generated as previously described (44). Eight- to 12-week-old mice were used in all experiments according to the guide for the care and use of laboratory animals (National Institutes of Health). NIH 3T3 cell cultures were maintained in Dulbecco's modified Eagle's medium supplemented with either 10% fetal bovine serum (FBS) or 0.5% FBS as indicated in the figure legends. The cells were cultured in a humidified environment containing 5% CO_2 at 37°C.

Plasmid construction. The retroviral expression vectors pLIRES-EGFP, pLIRES-EGFP-CA-NFAT1, CA-NFAT2, and pBabe-H-*rasV12* were used in the retroviral-transduction experiments. For more information on their construction, see the supplemental material. The CA-NFAT1ΔC truncated protein was constructed by mutation of CA-NFAT1 cDNA at sites C2205G and C2208T, creating a StuI restriction site just after the DBD by using the GeneTailor Site-Directed Mutagenesis system (Invitrogen). The mutated cDNA was then digested with StuI and NruI and religated, deleting the 227-amino-acid C terminus of NFAT1. The CA-NFAT1 construct contains a simian virus 40 nuclear localization signal at its C terminus adjacent to its stop codon, which was maintained. All CA-NFAT cDNAs were subcloned into pLIRES-EGFP. All constructs were confirmed by restriction enzyme mapping and DNA sequencing.

Production of recombinant retroviruses and infection of NIH 3T3 cells. The BD EcoPack2 ecotropic packaging cell line (BD Biosciences, San Jose, CA) was transiently transfected with retroviral vector by calcium phosphate precipitation for 24 h. The virus-containing cell supernatant was collected 48 h after transfection and concentrated using Amicon Ultracel 50k (Millipore, Billerica, MA). The supernatant was supplemented with 8 μg/ml Polybrene (Fluka Chemie, Buchs, Switzerland) and immediately used for spin infection (twice for 45 min each time at 380 × *g* at room temperature) of 2×10^4 NIH 3T3 cells. The infected cells were incubated at 37°C for an additional 24 h and trypsinized, and the efficiency of transduction was assessed by green fluorescent protein (GFP) expression using flow cytometric analyses. For CA-NFAT1 and CA-NFAT2 coexpression experiments, cells were first infected with CA-NFAT2-containing vector, expanded for 1 week, and then reinfected with CA-NFAT1 or empty vector. The efficiency of transduction was analyzed for CA-NFAT2 expression by GFP expression prior to the second round of infection and for CA-NFAT1 using intracellular staining with NFAT1 polyclonal antibody anti-67.1 and rhodamine-labeled anti-rabbit immunoglobulin G (KPL) by flow cytometric analyses. To ensure reproducibility, each experiment was repeated using cells derived from independent viral infections.

NIH 3T3–H-rasV12 cell construction. NIH 3T3–H-*rasV12* cells were generated by transducing NIH 3T3 wild-type cells with the pBabe-H-*rasV12* retroviral vector following selection for puromycin (15 μg/ml; Sigma) resistance for 14 days. Seven clones were then isolated and tested for H-*rasV12* expression by Western blotting (data not shown). All clones overexpressed H-*rasV12*, and one was selected for further experimentation.

Cell proliferation studies. NIH 3T3 wild-type or NIH 3T3–H-*rasV12* cells infected with either the control pLIRES-EGFP or pLIRES-EGFP-CA-NFAT virus were plated in triplicate in 96-well microtiter plates. For nonconfluent assays, 8×10^2 cells were plated per well; for confluent assays, 8×10^3 cells were plated per well. Cell proliferation was analyzed at the indicated times by crystal violet or [^{3}H]thymidine incorporation. The crystal violet incorporation assay involved fixing the cells with ethanol for 10 min, followed by staining them with 0.05% crystal violet in 20% ethanol for 10 min and solubilization with methanol. The plate was read on a spectrometer at 595 nm. The [^{3}H]thymidine incorporation assay consisted of pulsing the cells with [^{3}H]thymidine (5 μCi/ml) for 8 h. The cells were then harvested at the indicated times, and [^{3}H]thymidine incorporation was analyzed.

Cell cycle and sub-G_1 analyses. Six-well microtiter plates were inoculated with 2.4×10^4 or 2.4×10^5 cells for nonconfluence and confluence assays, respectively. On the indicated day, the cells were trypsinized and washed once with phosphate-buffered saline (PBS). The cells were then stained with propidium iodide (75 μM) in the presence of NP-40. Analysis of the DNA content was done by collecting 10,000 events for cell cycle analysis or 20,000 events for sub-G_1 analysis using a FACScalibur flow cytometer and CellQuest software (BD Biosciences).

Annexin V staining. NIH 3T3 cells infected with either pLIRES-EGFP or pLIRES-EGFP-CA-NFAT1 were plated at subconfluence densities, trypsinized 24 h later, washed with PBS, stained with phycoerythrin-conjugated annexin V (BD Biosciences), and analyzed by flow cytometry.

Focus formation. Infected NIH 3T3 or NIH 3T3–H-*rasV12* cells were diluted 1:5 or 1:500, respectively, with uninfected NIH 3T3 wild-type cells. These mixed cultures were plated at a final density of 5×10^4 cells/well of a six-well plate, and the growth medium was changed every 2 days. After 2 weeks, the cells were visualized by both phase-contrast microscopy and fluorescence microscopy for detection of GFP expression. Subsequently, the plates were rinsed in PBS and fixed with ethanol and then stained with 0.05% crystal violet in 20% ethanol to visualize foci.

Semisolid-medium growth and nude-mouse injections. Six-well plates were coated with 1.2% agarose-supplemented growth medium to resist cell adhesion. Infected or uninfected cells were then trypsinized, and 5×10^3 or 1×10^3 NIH 3T3 wild-type or H-*rasV12* cells, respectively, were resuspended in 3 ml of growth medium containing 0.6% agarose. After being plated, colonies were allowed to grow for 4 weeks for NIH 3T3 wild-type cells or for 2 weeks for NIH 3T3–H-*rasV12* cells. Representative colonies were visualized by both phase-contrast microscopy and fluorescence microscopy to detect GFP expression, and the total number of colonies was determined. For analysis of tumorigenic potential in vivo, uninfected cells or cells that had been infected with either the pLIRES-EGFP or the pLIRES-EGFP-CA-NFAT virus were trypsinized, washed, and resuspended in PBS. Athymic BALB/c nude mice were injected subcutaneously in the left flank with 5×10^5 NIH 3T3 wild-type cells or 3×10^5 NIH 3T3–H-*rasV12* cells, and tumor volumes (*V*) were analyzed every 5 days using the following formula: $V = 0.52 \times (\text{length}^2 \times \text{width})$. The numbers of mice that were injected with NIH 3T3 wild-type or H-*rasV12* cells, uninfected or infected with empty vector or CA-NFAT retroviruses, are indicated in the figure legends. Mice were sacrificed, and photographs were taken 70 days after injection for NIH 3T3 wild-type cells or 10 days after injection for NIH 3T3–H-*rasV12* cells.

MCA-induced tumor formation. Animals were injected subcutaneously in the hind flank with 50 μg/animal of methylcholanthrene (MCA) suspended in 0.1 ml sesame oil. Tumor development was observed weekly. Mice with a tumor >10 mm in diameter were counted as tumor positive and were sacrificed when they had an overt mass of ≥15 mm.

RESULTS

NFAT1 and NFAT2 sustained activity leads to opposite phenotypes when expressed in NIH 3T3 cells. In order to study the roles of NFAT transcription factors in cellular proliferation, we utilized well-characterized constitutively active CA-NFAT mutants (29, 31). CA-NFAT1 and CA-NFAT2 short isoform (CA-NFAT2/A) mutants were cloned into the retroviral vector pLIRES-EGFP. A schematic alignment of NFAT1 and NFAT2/A (short isoform) proteins is shown in Fig. 1A. Subsequent expression analysis of the encoded CA-NFATs demonstrated that the proteins functioned properly and had all the expected characteristics. NFAT mutant proteins transiently ex-

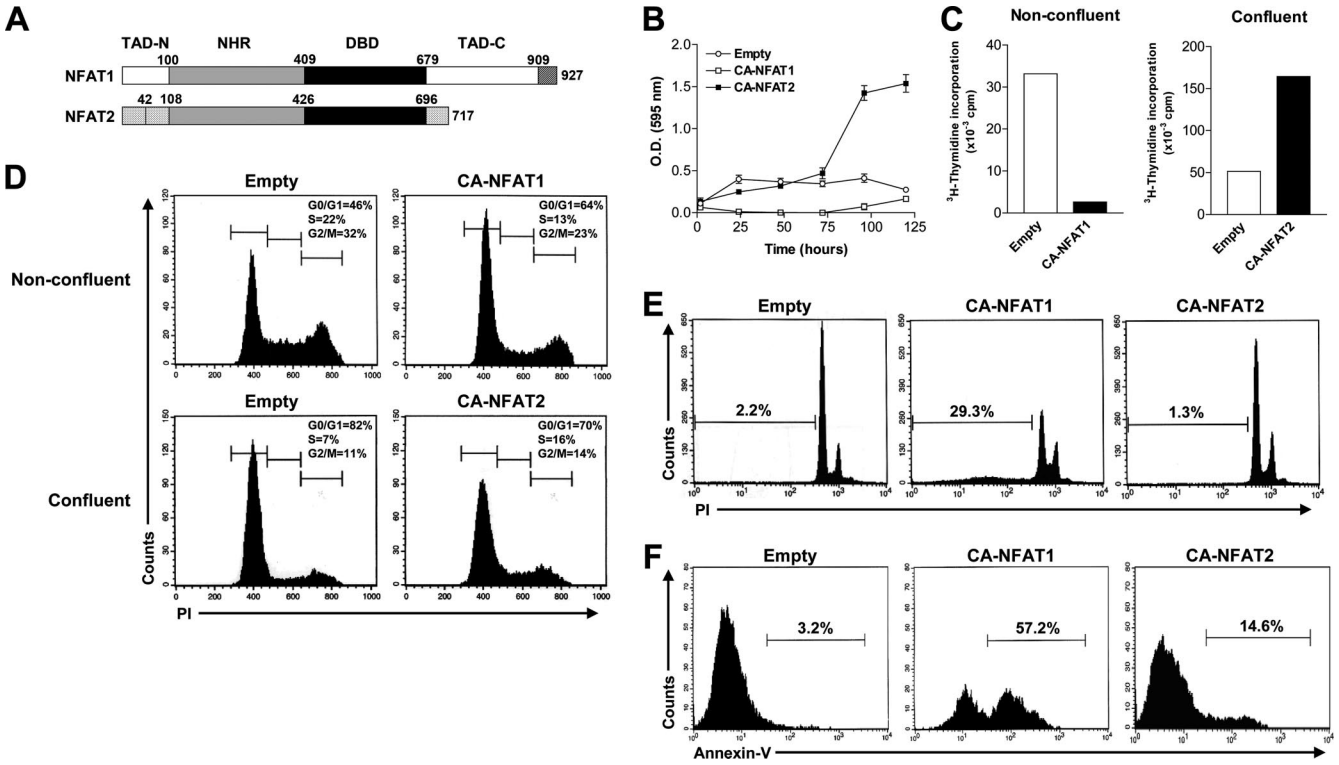

FIG. 1. NFAT1 and NFAT2 sustained activity induces opposite phenotypes in NIH 3T3 cells. Cells were infected with the empty vector or CA-NFAT1 or CA-NFAT2 retrovirus, plated at the indicated confluence, and analyzed for cell growth, cycle, and death. (A) Schematic alignment of NFAT proteins used in the study. TAD, transactivation domain. For protein isoforms, identical shading patterns represent identical sequences. The boundary of each region is labeled above the sequence, with the numbering referring to the amino acid position of the murine protein. (B) Proliferation kinetic analyses by crystal violet staining. O.D., optical density. (C) Cell proliferation after a 24-h period analyzed by [^{3}H]thymidine incorporation. (D) Cell cycle analysis 48 h after plating. Cells were fixed and stained with propidium iodide (PI) and then analyzed by flow cytometry. The percentage of cells in each stage of the cell cycle (G_0/G_1, S, and G_2/M) is indicated. (E) Cell death analysis. Cells were plated at confluence and then were stained with PI and analyzed by flow cytometry 48 h after being plated. The percentages of cell death (sub-G_0) are indicated. (F) Cells were plated at confluence and then were stained with annexin V and analyzed by flow cytometry 24 h later. The percentages of phosphatidylserine-positive cells are indicated. All results are representative of at least three independent experiments. The standard deviations (error bars) indicate the variance within one experiment.

pressed in HEK293 cells had the expected apparent molecular weight, were constitutively localized in the nucleus compared to wild-type NFAT proteins, and when expressed in Jurkat T cells, CA-NFAT proteins showed the capability to constitutively transactivate an NFAT-responsive reporter luciferase construct (3xNFAT-Luc) compared to wild-type NFATs (see Fig. S1 in the supplemental material). All constructs showed similar infection capabilities, protein expression, protein nuclear localization, and transactivation activities (data not shown), validating their use in elucidating the mechanism behind the observed differences between NFAT1 and NFAT2 in regulating cell proliferation. Retroviral transduction was used, and >85% of NIH 3T3 cells were routinely infected. High levels of infection allow the analysis of the bulk-infected population of cells, preventing any possible cell alteration caused by isolating cell line clones.

When we first infected NIH 3T3 cells with CA-NFAT cDNAs or pLIRES-EGPF empty vector, we noticed a striking difference between the cultures. Whereas NIH 3T3 wild-type cells and cells infected with empty vector (control) showed similar cell densities and viabilities, CA-NFAT2-expressing cells had increased in numbers, a characteristic opposite of CA-NFAT1-expressing cells, which demonstrated a remarkable reduction in total cell number and viability as analyzed by trypan blue exclusion (data not shown). To further analyze this difference in growth capacity, we performed a proliferation-kinetics assay accompanied by crystal violet incorporation, which correlates with total cell numbers. Unlike control cells, which stopped growing once they had reached confluence, we found that CA-NFAT2-expressing cells overgrew the monolayer and continued to proliferate beyond confluence (Fig. 1B). Surprisingly, CA-NFAT1-expressing cells showed a completely opposite phenotype. They did not reach confluence, accumulated in reduced numbers, and kept a low proliferation profile throughout the experiment (Fig. 1B). In fact, NIH 3T3 cells expressing CA-NFAT1 showed a remarkable reduction in cell proliferation and were predominantly in the G_1 phase of the cell cycle after a 48-h period compared to the control (Fig. 1C and D). In contrast, we found that CA-NFAT2-expressing cells continued to proliferate in an overconfluent culture and maintained a cell cycle profile typical of actively dividing cells (Fig. 1C and D). These data suggest that NFAT1 and NFAT2 have different roles in the control of cell growth and proliferation.

Since CA-NFAT1-expressing cells appeared to suffer a re-

duction in numbers in the proliferation-kinetics assay, we next assessed the involvement of cell death. NIH 3T3 cells infected with empty vector exhibited a low proportion of cells having sub-G_0 DNA content, as shown by flow cytometry, indicative of cells undergoing apoptosis (Fig. 1E). This low level of cell death was also seen in CA-NFAT2-expressing cells (Fig. 1E). However, 72 h after the cells were infected with CA-NFAT1, approximately one- third of the cells exhibited sub-G_0 DNA content, indicating that CA-NFAT1 induced apoptosis in NIH 3T3 cells (Fig. 1E). Annexin V staining of CA-NFAT1-expressing cells 48 h postinfection showed that DNA fragmentation is preceded by an externalization of phosphatidylserine, confirming that CA-NFAT1 is capable of inducing apoptosis in NIH 3T3 cells (Fig. 1F), while control NIH 3T3 cells expressing empty vector or CA-NFAT2 showed only a low level of annexin V staining (Fig. 1F). Taken together, these results indicate that sustained activation of the NFAT1 signaling pathway inhibits the cell cycle and induces apoptosis, as reflected by the decrease in total cell numbers. However, this phenotype is completely opposite to the one induced by sustained activation of NFAT2, which leads to cell accumulation.

CA-NFAT2 activity, but not CA-NFAT1 activity, is able to induce all transformation hallmarks in NIH 3T3 cells. We next asked whether CA-NFAT2 is able to induce a transformed phenotype in NIH 3T3 cells. We previously observed that CA-NFAT2-expressing NIH 3T3 cells exhibit growth beyond confluence, which indicates loss of contact growth inhibition. To better visualize this phenotype, we performed a focus-forming assay in which empty-vector control or CA-NFAT-expressing cells were plated together with an excess of uninfected NIH 3T3 wild-type cells. Next, the cells were grown in culture for 12 to 15 days, and formation of transformed foci was analyzed by crystal violet staining and fluorescence microscopy. Control empty-vector- and CA-NFAT1-infected cells gave rise to only a small number of small foci when analyzed by crystal violet staining, suggesting that these two constructs are not able to transform NIH 3T3 cells (Fig. 2A). However, when CA-NFAT2 was expressed in these cells, a large number of foci formed (Fig. 2A). Since GFP and CA-NFATs were expressed from the same bicistronic mRNA in the pLIRES-EGFP vector, we were able to track cells that expressed CA-NFATs or the empty vector, directly discriminating them from NIH 3T3 wild-type cells by fluorescence microscopy. From this analysis, we found that cells infected with empty vector were morphologically indistinguishable from uninfected neighboring cells (data not shown). Furthermore, most of the foci formed in empty-vector-treated cells were GFP negative, indicating that focus formation in this culture was due to spontaneous transformation of NIH 3T3 cells, rather than to retroviral transduction (Fig. 2B). Also, foci formed in the CA-NFAT1-infected culture did not show GFP fluorescence, confirming that CA-NFAT1 is not able to transform NIH 3T3 cells (Fig. 2B). However, all of the CA-NFAT2-expressing cells in the mixed culture formed readily detectable GFP-bright foci (Fig. 2B).

To further analyze the cell-transforming potential of CA-NFAT proteins, NIH 3T3 cells were plated in semisolid agarose medium, in which there is no solid substratum for cell adhesion to occur. CA-NFAT2-expressing cells readily formed many large, GFP-bright colonies compared to control cells (Fig. 2C and D). Conversely, CA-NFAT1 and control empty-vector-expressing cells formed only a few small colonies (Fig. 2C and D). In the case of CA-NFAT1-infected cells, none of the colonies formed were fluorescent, and thus, they were likely formed by uninfected NIH 3T3 cells, indicating that CA-NFAT1 suppresses colony formation, as well as being unable to transform NIH 3T3 cells (Fig. 2D).

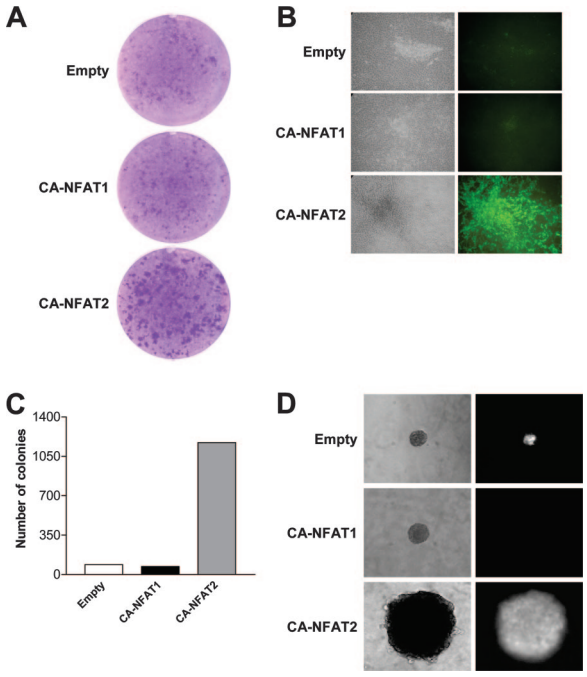

FIG. 2. NFAT2, but not NFAT1, constitutive activity is able to transform NIH 3T3 cells. NIH 3T3 cells were infected with empty vector or CA-NFAT1 or CA-NFAT2 retrovirus. (A) Cells transduced with the indicated constructs were mixed 1:5 with uninfected NIH 3T3 wild-type cells and grown to 15 days postconfluence. Focus formation was assessed by crystal violet staining. (B) Phase-contrast microscopy (left) and optical fluorescence microscopy for GFP expression (right) of representative NIH 3T3 foci from panel A. (C) Quantitation of colonies from NIH 3T3 cells infected with either empty vector or CA-NFAT retroviruses grown in semisolid agarose medium. Cells (5×10^3) were inoculated, and colonies were counted 30 days after being plated. (D) Phase-contrast microscopy (left) and optical fluorescence microscopy for GFP expression (right) of representative NIH 3T3 colonies from panel C. All results are representative of at least three independent experiments.

Furthermore, we tested whether CA-NFAT2 could affect cell proliferation under reduced-serum conditions, which are known to induce cell cycle arrest and apoptosis in normal fibroblasts. When cultured in 0.5% FBS medium, control NIH 3T3 cells failed to grow and exhibited a reduced proliferation rate (Fig. 3A and B). Additionally, a large proportion of control cells had sub-G_0 DNA content, indicative of apoptosis, and a low accumulation of cells in the G_1 phase of the cell cycle (Fig. 3C and D). Remarkably, NIH 3T3 cells expressing CA-NFAT2 showed the ability to grow under serum starvation conditions, exhibited high levels of cell proliferation, and were able to enter the cell cycle, as shown by a moderate increase in cells in the S and G_2/M phases of the cell cycle (Fig. 3A to C). More surprisingly, CA-NFAT2-treated cells were able to prevent growth factor withdrawal-induced apoptosis (Fig. 3D).

As a final confirmation of the transforming potential of

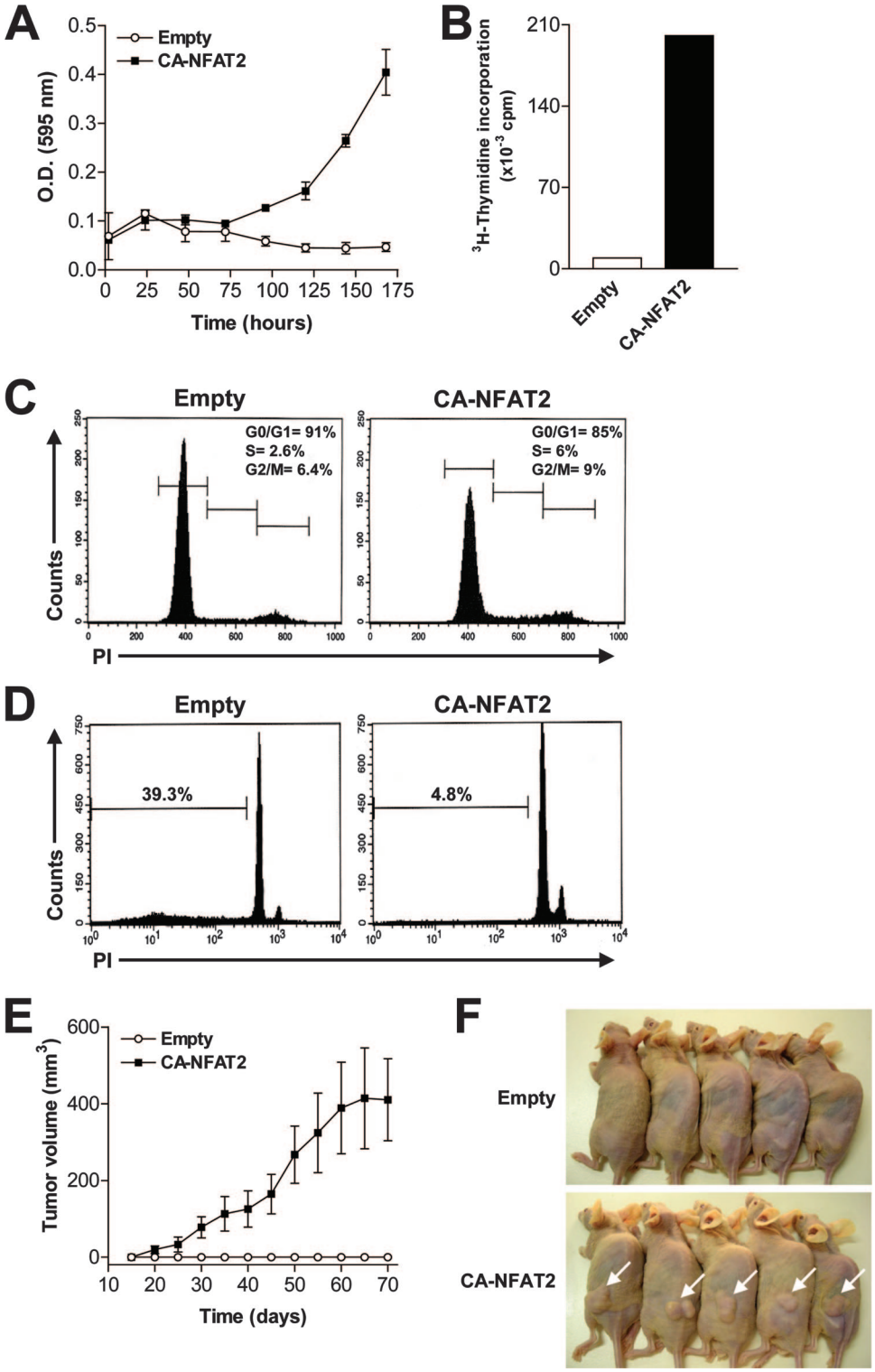

FIG. 3. Sustained NFAT2 activity in NIH 3T3 cells promotes cell cycle progression and prevents apoptosis under reduced-serum conditions and induces the formation of tumors in athymic nude mice. NIH 3T3 wild-type cells were infected with either empty vector or CA-NFAT2 retrovirus. (A and B) Infected cells were plated in triplicate, and cell proliferation was determined by incorporation of crystal violet (A) or by [^{3}H]thymidine incorporation (B) 144 h after plating. O.D., optical density. (C) Cell cycle analysis of infected cells 144 h after being plated. Cells were analyzed as for Fig. 1D. (D) Cell death analysis 144 h after plating. Cells were analyzed as for Fig. 1E. (A to D) Cells were cultured at confluence under reduced-serum conditions (0.5% [vol/vol] FBS). The results are representative of at least three independent experiments. The standard deviations (error bars) indicate the variance within one experiment. (E and F) Tumor formation in nude mice following subcutaneous injection of 5×10^5 cells infected with empty vector ($n = 6$) or CA-NFAT2 ($n = 7$). (E) Tumor volumes were measured every 5 days, and the data are shown as means $\pm$ standard errors of the mean. (F) Tumors from five representative mice are indicated by white arrowheads.

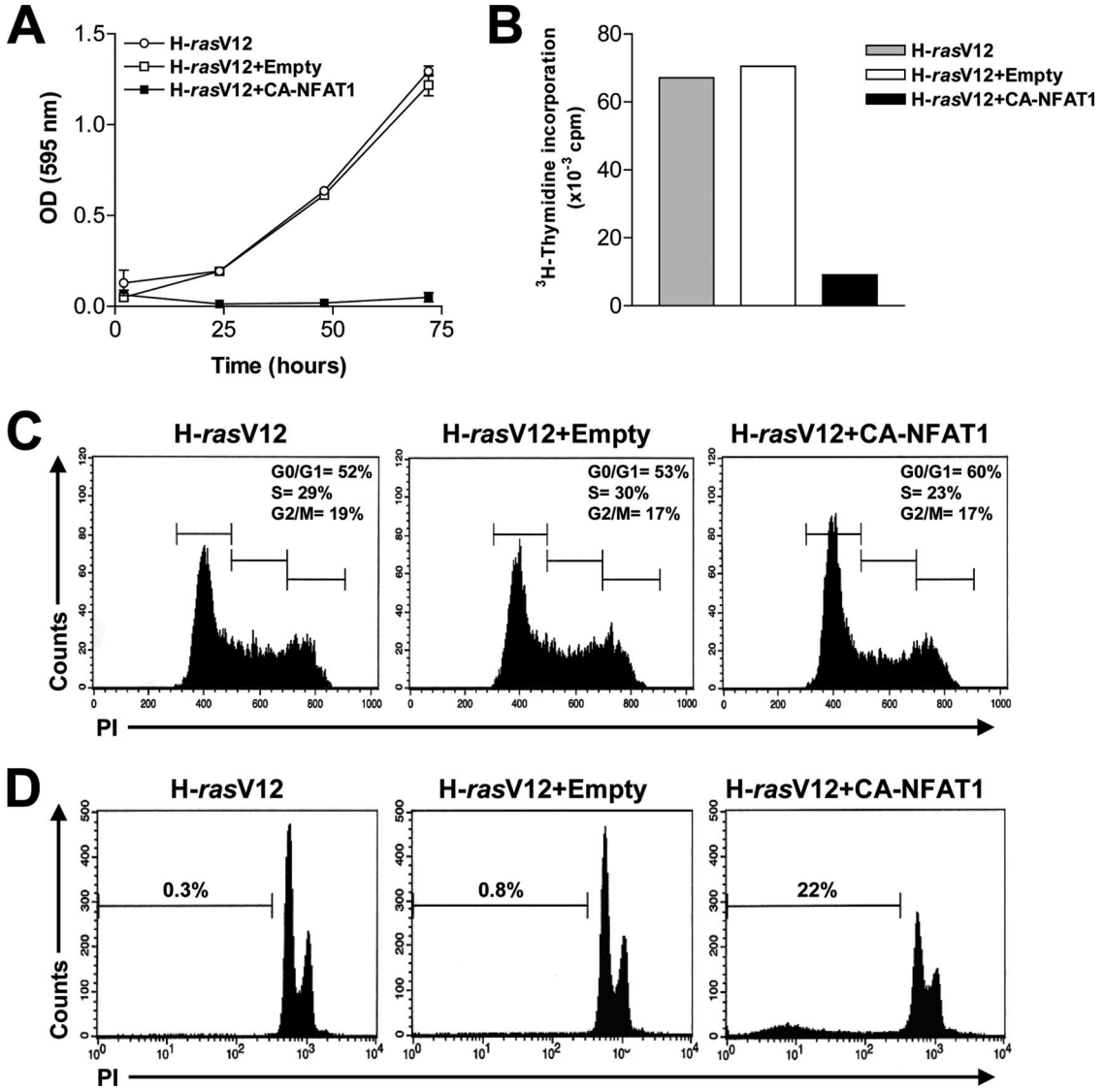

FIG. 4. CA-NFAT1 suppresses cell proliferation and induces death in neoplastic cells. NIH 3T3–H-*rasV12* cells, uninfected or infected with either the empty vector or CA-NFAT1 retrovirus, were plated, and cell growth, cycle, and death were analyzed as for Fig. 1. (A and B) Cells were analyzed for proliferation daily by incorporation of crystal violet (A) or in a nonconfluent manner after a 48-h period by [^{3}H]thymidine incorporation (B). OD, optical density. (C) Cell cycle analysis 48 h after plating at subconfluence. (D) Cell death analysis 48 h after plating at confluence. All results are representative of at least three independent experiments.

CA-NFAT2, we tested whether the protein was able to induce tumor formation in athymic nude mice. NIH 3T3 cells expressing empty vector or CA-NFAT2 protein were implanted in the flanks of BALB/c nude mice, and the animals were monitored for tumor formation. Whereas all mice inoculated with CA-NFAT2-expressing cells displayed large flank tumors that continued to grow with time, none of the mice inoculated with control cells exhibited detectable tumors, even 70 days after inoculation (Fig. 3E and F). Taken together, these results clearly highlight the oncogenic potential of NFAT2 and suggest a unique role for the protein, whereas the NFAT1 protein appears unable to induce the transformed phenotype.

Sustained NFAT1 activity shows tumor suppressor capability. We have previously shown that lymphocytes from NFAT1-deficient mice have a hyperproliferative phenotype that correlates with an overexpression of cyclins A2, B1, E, and F (6). Ranger et al. also demonstrated that these mice have a propensity to develop cartilage neoplastic transformation (37). These data suggest that NFAT1 might be a negative regulator of cell proliferation and transformation, which correlates with our results in NIH 3T3 cells. To directly test whether NFAT1 has the capability to suppress cell growth and to subvert a transformed cell phenotype, we constructed NIH 3T3 cell clones that harbor the oncogene H-*rasV12* (NIH 3T3–H-*rasV12*). Analysis of the NIH 3T3–H-*rasV12* clones showed the typical transformed phenotype, and one clone was chosen for further experiments (data not shown). Subsequently, we tested whether CA-NFAT1 was able to suppress these transformed characteristics of the NIH 3T3–H-*rasV12* clone. As shown in Fig. 4A, NIH 3T3-H-*rasV12* cells, uninfected or infected with

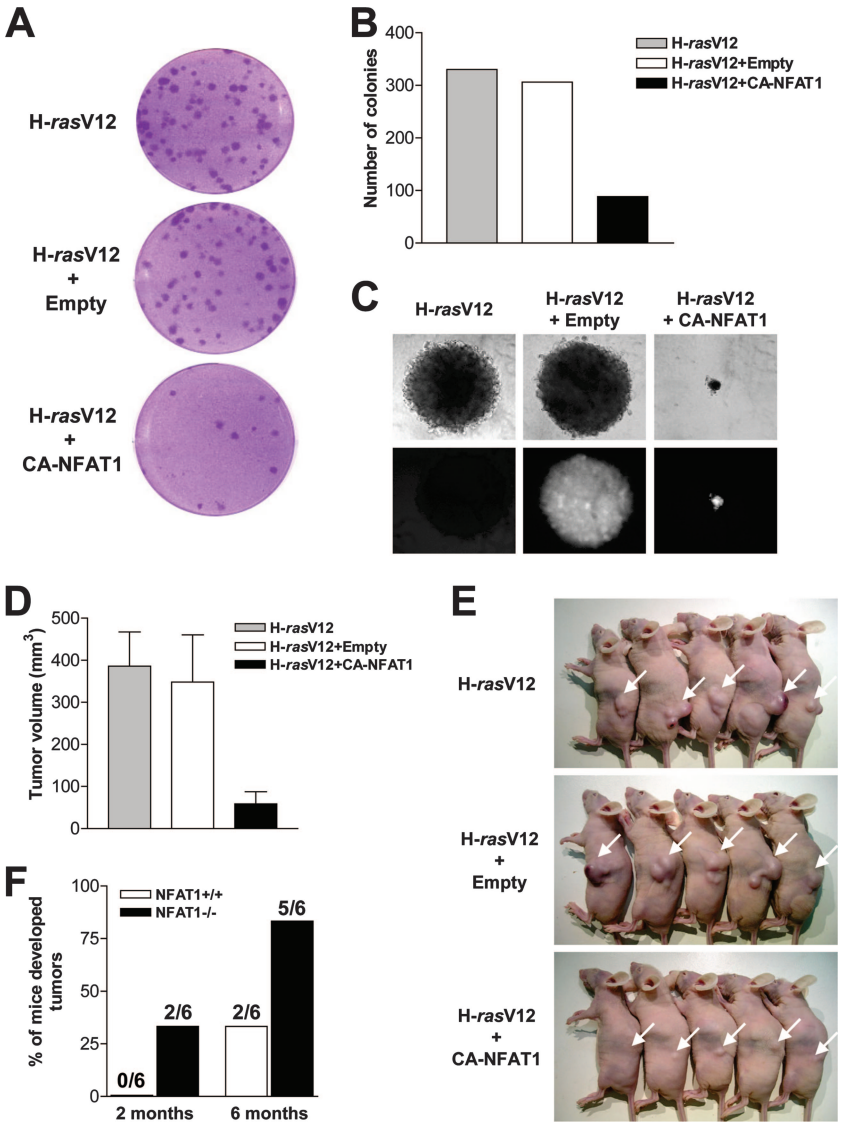

FIG. 5. CA-NFAT1 acts as a tumor suppressor gene. (A to E) NIH 3T3–H-*rasV12* cells were infected with the empty vector or CA-NFAT1 retrovirus. (A) NIH 3T3–H-*rasV12* cells transduced with the indicated constructs were mixed 1:500 with uninfected NIH 3T3 wild-type cells and grown to 15 days postconfluence. Focus formation was assessed by crystal violet staining. (B) Quantitation of colonies from transformed cells grown in semisolid agarose medium. Cells (1×10^3) were inoculated, and colonies were counted 2 weeks after being plated. (C) Phase-contrast microscopy (top) and optical fluorescence microscopy for GFP expression (bottom) of representative NIH 3T3–H-*rasV12* colonies from panel B. These results are representative of at least three independent experiments. (D and E) Tumor formation in nude mice following subcutaneous injection of 3×10^5 NIH 3T3–H-*rasV12* ($n = 7$)-, NIH 3T3–H-*rasV12*–empty vector ($n = 7$)-, or NIH 3T3–H-*rasV12*–CA-NFAT1 ($n = 5$)-expressing cells. Tumor volumes were measured every 5 days. (D) The data are shown as means plus standard errors of the mean. (E) Tumors from five representative mice are indicated by white arrowheads. (F) Susceptibilities of NFAT1$^{+/+}$ and NFAT1$^{-/-}$ mice to chemical carcinogen-induced tumors. The animals were injected subcutaneously with a single dose of MCA and evaluated for the occurrence of tumors at the indicated times. The data are expressed as the percentage of the number of mice that developed tumors ($n = 6$).

empty vector, grew similarly. However, CA-NFAT1 expression was able to reduce the cell growth of the transformed NIH 3T3–H-*rasV12* cells throughout the time course. This reduction in growth was accompanied by a large decrease in DNA replication and an accumulation in G_1 phase of the cell cycle after a 48-h period postinfection compared to control cells (Fig. 4B and C). CA-NFAT1 expression in NIH 3T3–H-*rasV12* cells also induced these transformed cells to undergo apoptosis, as indicated by sub-G_0 DNA content analysis, which was not seen in empty-vector-expressing cells (Fig. 4D).

We next asked whether the CA-NFAT1 cell cycle arrest and cell death induction could lead to a reversion of other hallmarks of cellular transformation. Indeed, CA-NFAT1 expression in NIH 3T3–H-*rasV12* was able to clearly reduce the number of foci formed in culture compared to NIH 3T3–H-*rasV12* and empty-vector-expressing cells that immediately formed foci (Fig. 5A). Additionally, the foci formed in CA-NFAT1-expressing cells were negative for GFP when analyzed by fluorescence microscopy, indicating that they were formed by nontransduced cells (data not shown). Further, NIH 3T3–

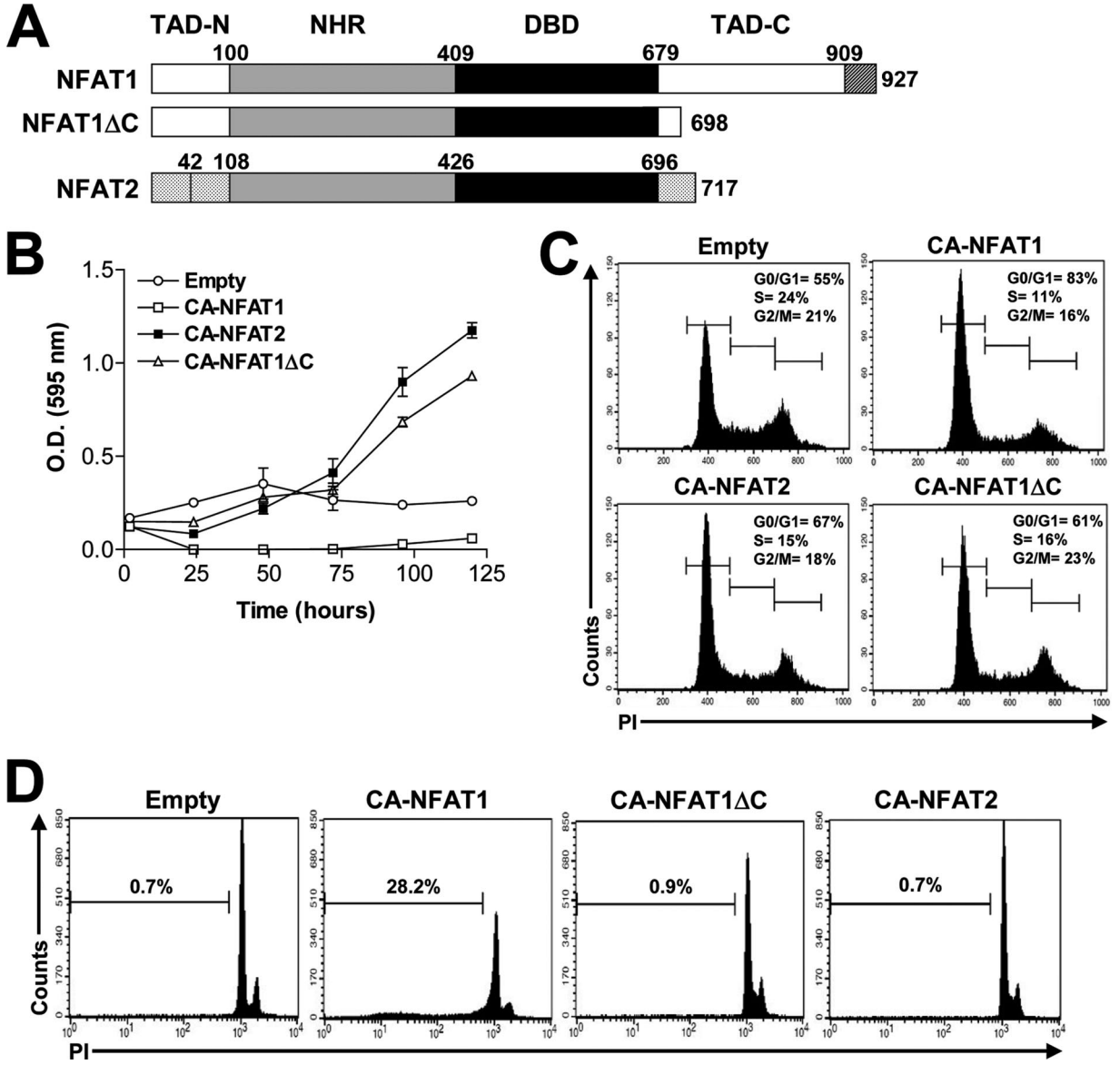

FIG. 6. Deletion of the long C terminus disrupts the ability of CA-NFAT1 to induce apoptosis and cell cycle arrest. (A) Schematic alignment of wild-type NFATs and truncated NFAT1ΔC proteins. See the legend to Fig. 1A for details. (B to D) Cells were infected with either the empty vector or CA-NFAT1, CA-NAFT1ΔC, or CA-NFAT2 retrovirus. The cells were plated, and then cell growth, cycle, and death were analyzed as for Fig. 1. (B) Cells were analyzed for proliferation daily by incorporation of crystal violet. O.D., optical density. The error bars indicate standard deviation. (C) Cell cycle analysis 48 h after plating at subconfluence. PI, propidium iodide. (D) Cell death analysis 48 h after plating at confluence. All results are representative of at least three independent experiments.

H-*rasV12* CA-NFAT1-expressing cells formed only a few small colonies in semisolid medium compared to controls (Fig. 5B and C). GFP expression analysis showed that almost all colonies in empty-vector-expressing cells were fluorescent, which was seen only in very small colonies in the CA-NFAT1-expressing culture (Fig. 5C). Furthermore, we inoculated NIH 3T3–H-*rasV12* cells infected or uninfected with control or CA-NFAT1 retroviruses in the flanks of BALB/c nude mice. Although the transformation phenotype induced by the H-*rasV12* oncogene in NIH 3T3 cells is strong, the constant CA-NFAT1 expression and signaling clearly reduced the size of the tumors formed in athymic mice (Fig. 5D and E).

We had shown that CA-NFAT1 is able to subvert the transformed phenotype of NIH 3T3 induced by the H-*ras*V12 oncogene. Next, we tested whether the lack of NFAT1 expression was able to increase the rate of tumor formation in NFAT1-deficient mice. Thus, wild-type (+/+) or NFAT1-deficient (−/−) mice were injected subcutaneously with a single dose of MCA and tumor occurrence was evaluated at the indicated times. While no wild-type mice developed tumors after 2 months and only 30% developed tumors after a 6-month period, 33% of NFAT1-deficient mice promptly developed sarcomas and approximately 80% of the mice developed tumors 6 months after MCA injection (Fig. 5F). This result demon-

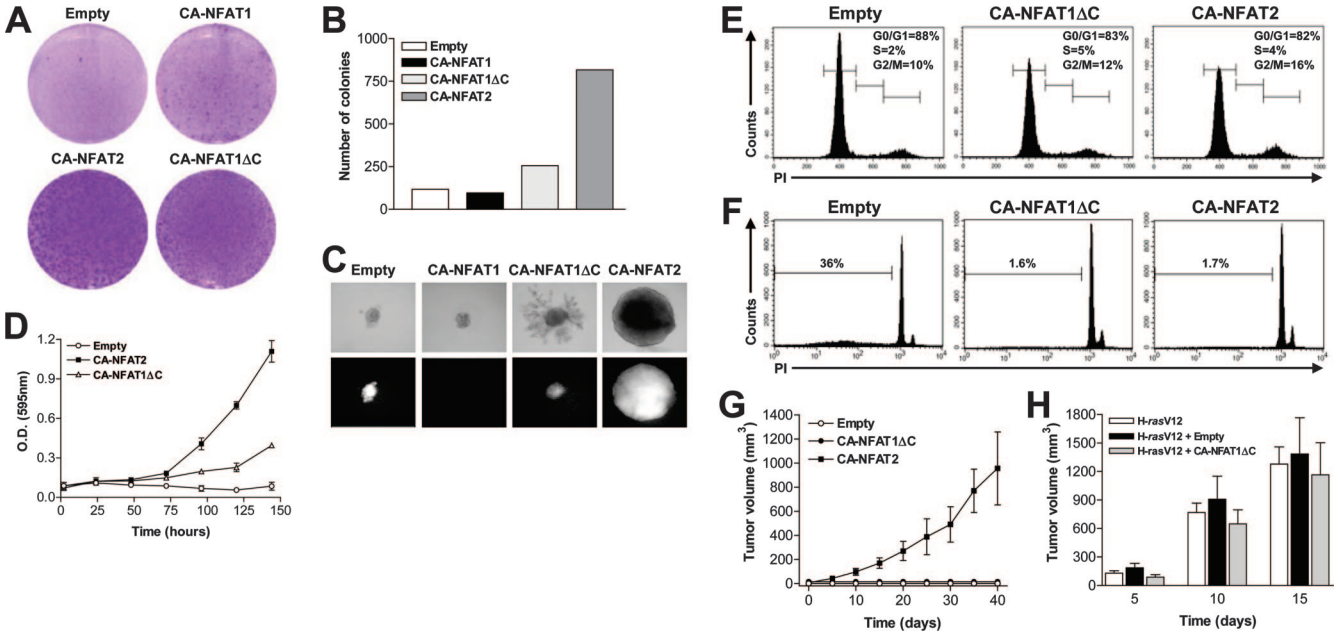

FIG. 7. Truncated CA-NFAT1 protein lacking the C terminus induces an intermediate transformed phenotype. NIH 3T3 cells infected with either the empty vector or CA-NFAT1, CA-NFAT1ΔC, or CA-NFAT2 retrovirus were used for all experiments. Infected cells were cultured in medium containing 10% FBS (A to C) or to subconfluence in the presence of 0.5% FBS (D to F). Focus formation (A) and semisolid-medium growth (B and C) were assessed as for Fig. 2. (C) Phase-contrast microscopy (top) and optical fluorescence microscopy for GFP expression (bottom) of representative NIH 3T3 colonies from panel B. (D) Infected cells were plated in triplicate, and cell proliferation was determined daily by incorporation of crystal violet. (E) Cell cycle analysis of infected cells 144 h after being plated in reduced serum concentrations (0.5%). The cells were analyzed as for Fig. 1D. (F) Cell death analysis 144 h after being plated in reduced serum concentration (0.5%). The cells were analyzed as for Fig. 1E. All results are representative of at least three independent experiments. (G) Tumor formation in nude mice following subcutaneous injection of 5×10^5 NIH 3T3-empty vector ($n = 5$)-, CA-NFAT1ΔC ($n = 5$)-, or CA-NFAT2 ($n = 5$)-expressing cells. Tumor volumes were measured every 5 days, and the data are shown as means ± standard errors of the mean (SEM). (H) Tumor formation in nude mice following subcutaneous injection of 3×10^5 NIH 3T3–H-*rasV12* ($n = 5$)-, NIH 3T3–H-*rasV12*–empty vector ($n = 5$)-, or NIH 3T3–H-*rasV12*–CA-NFAT1ΔC ($n = 5$)-expressing cells. Tumor volumes were measured every 5 days. The data are shown as means plus SEM.

strates that the lack of NFAT1 predisposes these mice to develop tumors under the action of chemical carcinogens and, taken together with the in vitro data in NIH 3T3 cells, suggests a tumor suppressor role for the NFAT1 protein.

The NFAT1 carboxy terminus is responsible for the tumor suppressor phenotype. To further investigate the different roles of NFAT proteins in the control of the cell cycle and death, a schematic analysis of a primary sequence alignment of murine NFAT1 and NFAT2/A cDNAs was created and is shown in Fig. 6A. As can be readily seen, NFAT1 has a long C terminus that is present in all NFAT family members (data not shown), with some variation in its primary sequence. However, this C terminus is completely absent in NFAT2/A due to an early poly(A) site downstream of exon 9 (10). We next sought to determine whether the NFAT1 C-terminal domain could be responsible for the differences observed between the NFAT1 and NFAT2 proteins. To answer this question, we constructed a truncated NFAT1 protein that lacked the long C terminus (NFAT1ΔC) by making a deletion a few amino acids after its DBD. The resulting mutant resembled the short C terminus of NFAT2/A (Fig. 6A). Strikingly, in a proliferation time course, CA-NFAT1ΔC-expressing NIH 3T3 cells showed a phenotype completely different from that of NIH 3T3 cells expressing the full-length CA-NFAT1 protein (Fig. 6B). Whereas CA-NFAT1 induced a reduction in cell growth compared to control cells, CA-NFAT1ΔC-expressing cells showed overconfluent growth capability almost reaching CA-NFAT2 levels (Fig. 6B). In an NIH 3T3 cell culture, CA-NFAT1 expression induced a slight cell cycle arrest and significant apoptosis compared to controls, as evident in the increase of the G_1 phase of the cell cycle and the sub-G_0 DNA content, respectively, compared to the control (Fig. 6C and D). Conversely, the deletion of the NFAT1 C terminus (CA-NFAT1ΔC) was sufficient to completely abolish these phenotypes and to induce a CA-NFAT2-like phenotype.

Since CA-NFAT1ΔC was able to induce overconfluent proliferation indicative of loss of contact growth inhibition and showed characteristics of CA-NFAT2/A-expressing cells, we next determined whether the protein was also able to induce other transformation phenotypes. As shown in Fig. 7A, CA-NFAT1ΔC was able to readily induce focus formation in culture, although these foci were smaller than those formed by CA-NFAT2-expressing cells (Fig. 7A). Furthermore, when we analyzed the NIH 3T3 cell colony formation in a semisolid medium, CA-NFAT1 was unable to induce colony formation, while CA-NFAT1ΔC expression was able to double the number of colonies formed compared to empty-vector-expressing cells (Fig. 7B). Once again, the colonies formed by CA-NFAT1ΔC-expressing cells were less abundant and smaller than those of CA-NFAT2-expressing NIH 3T3 cells (Fig. 7B and C). As a final test, we analyzed the cell growth capacity under reduced serum conditions. CA-NFAT1ΔC-expressing

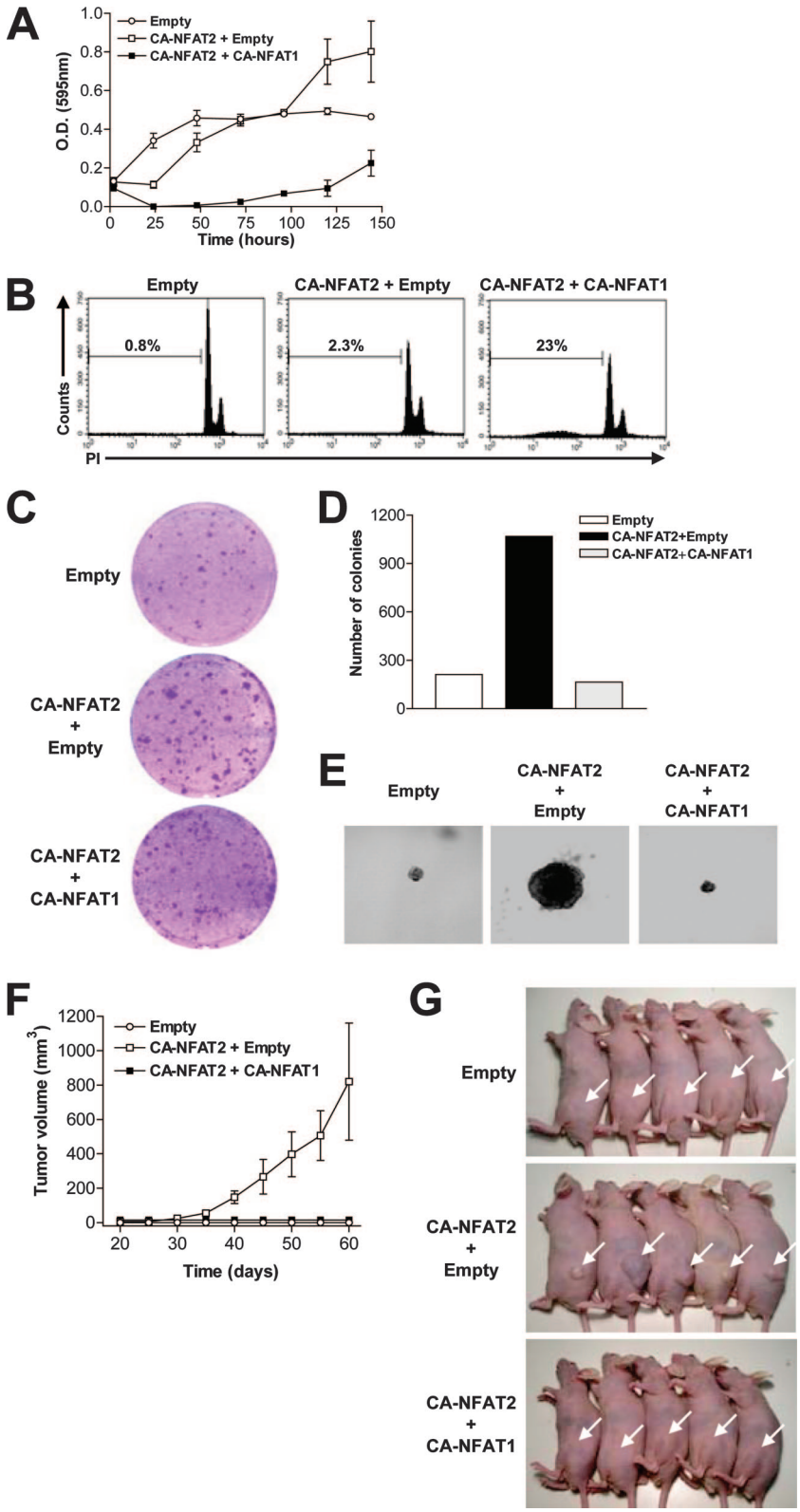

FIG. 8. CA-NFAT1 suppresses the transformed phenotype induced by CA-NFAT2. NIH 3T3 cells were infected with CA-NFAT2 (NIH 3T3–CA-NFAT2), and 1 week later, the cells were reinfected with empty vector or CA-NFAT1. Then, 24 h after the second round of infection, the cells were plated (0 h) and analyzed at the indicated times for proliferation daily by incorporation of crystal violet as for Fig. 1B (A), for cell death 48 h after being plated at confluence as for Fig. 1E (B), for focus formation by crystal violet staining as for Fig. 2A (C), for colony formation in semisolid medium as for Fig. 2C and D (D and E), and for tumor formation in nude mice following subcutaneous injection of 5×10^5 NIH 3T3-empty vector ($n = 5$)-, NIH 3T3–CA-NFAT2 plus empty vector ($n = 5$)-, or NIH 3T3–CA-NFAT2 plus CA-NFAT1 ($n = 5$)-expressing cells as for Fig. 3E and F (F and G). (F) Tumor volumes were measured every 5 days. The data are shown as means ± standard errors of the mean. (G) Tumors from five representative mice are indicated by white arrowheads. All results are representative of at least three independent experiments.

NIH 3T3 cells cultivated in 0.5% FBS medium showed intermediate cell growth compared to that of CA-NFAT2- and empty-vector-expressing cells (Fig. 7D). When these cells were analyzed after a 6-day culture period in 0.5% FBS medium, CA-NFAT1ΔC-expressing cells showed a proliferation profile similar to that of CA-NFAT2-expressing cells with a moderate decrease of cells entering the G_2/M phase of the cell cycle (Fig. 7E). Remarkably, CA-NFAT1ΔC expression in NIH 3T3 cells was able to protect the cells from apoptosis induced by growth factor withdrawal compared to empty-vector-expressing cells (Fig. 7F).

We next assessed the capacity of CA-NFAT1ΔC to promote tumor growth (Fig. 7G). While NIH 3T3 cells expressing CA-NFAT2 formed readily detectable tumors upon injection into BALB/c nude mice, empty-vector- and CA-NFAT1ΔC-expressing cells failed to do so for the length of the experiment (Fig. 7G), even up to 80 days postinjection (data not shown). Nevertheless, CA-NFAT1ΔC did not repress tumor growth of NIH 3T3–H-*rasV12*-transformed cells compared to wild-type and empty-vector-expressing NIH 3T3–H-*rasV12* cells (Fig. 7H). Taken together, these data indicate that the C-terminal domain of NFAT1 is responsible for the proapoptotic, cell cycle arrest, and tumor suppressor characteristics of the protein. Moreover, deletion of the NFAT1 C-terminal domain confers a partial cell transformation phenotype that resembles the phenotype induced following NFAT2/A protein expression.

CA-NFAT1 suppresses CA-NFAT2-induced transformation. Since sustained activation of NFAT1 was able to subvert cell transformation by the strong oncogene H-*rasV12*, we next asked what was the effect of CA-NFAT1 on the CA-NFAT2-transformed NIH 3T3 cells. We addressed this question by infecting NIH 3T3 cells with empty vector or CA-NFAT2 and 1 week later reinfecting these cells with either empty vector or CA-NFAT1. Both CA-NFAT1 and CA-NFAT2 vectors carry the GFP gene as the reporter gene; therefore, we confirmed the first round of infections by analysis of GFP expression and the second through intracellular staining for NFAT1. In fact, about 85% of CA-NFAT2-infected NIH 3T3 cells were GFP bright after the first infection whereas about 83% expressed NFAT1 after the second round. As shown for CA-NFAT2-expressing NIH 3T3 cells (Fig. 1 to 3), NIH 3T3–CA-NFAT2 cells infected with empty vector displayed an overgrowth phenotype (Fig. 8A), normal levels of cell death (Fig. 8B), loss of contact growth inhibition (Fig. 8C), a capacity for colony formation in a semisolid substrate (Fig. 8D and E), and the ability to form tumors when injected in BALB/c nude mice compared to control cells (Fig. 8F and G). These results demonstrate that cells were still transformed after the second round of infection and after the time elapsed from the first infection. Distinctively, NIH 3T3–CA-NFAT2 cells infected with CA-NFAT1 exhibited a dramatic reduction in cell numbers and a low rate of proliferation compared to controls (Fig. 8A). The reduction in cell numbers was at least partially accounted for by increased cell death (Fig. 8B). Furthermore, CA-NFAT1 expression by NIH 3T3–CA-NFAT2 cells was able to reduce the size and the number of foci in focus-forming assays (Fig. 8C) and colonies in semisolid medium (Fig. 8D and E), suggesting a reversal of the transformed phenotype induced by CA-NFAT2. Finally, the expression of CA-NFAT1 by NIH 3T3–CA-NFAT2 completely abolished in vivo tumor formation upon inoculation into BALB/c nude mice (Fig. 8F and G). Together, these data demonstrate that NFAT1 signaling is sufficient to abolish the transformation potential of NFAT2 short isoform.

DISCUSSION

In the current study, we showed that sustained activity of NFAT family members, NFAT1 and NFAT2, is able to regulate different mechanisms involved in the growth and death of NIH 3T3 fibroblasts (Fig. 1). The CA-NFAT2 short isoform induces a strong transformation phenotype, whereas CA-NFAT1 suppresses cell growth, apparently through its C-terminal domain. We showed that CA-NFAT2 short isoform is sufficient to induce NIH 3T3 cells to acquire the well-established hallmarks of cellular transformation that define it as a possible oncogene (Fig. 2 and 3) (17). However, CA-NFAT1 shows an antioncogenic activity. It was proposed that a candidate tumor suppressor gene should subvert the transformation phenotype when reintroduced into neoplastic cells and that the absence of the tumor suppressor gene in a cell or an animal should lead to an increased propensity to acquire a transformed phenotype (27). Our data directly show these characteristics for CA-NFAT1 and strongly suggest that NFAT1 is a tumor suppressor gene (Fig. 4 and 5). Moreover, CA-NFAT1 was able to suppress the transformed phenotype induced by CA-NFAT2 short isoform (Fig. 8), suggesting that different family members might have complementary functions and that the balanced expression of the two proteins might be important for the cell to enter into programs that determine whether it will live, proliferate, or die. Furthermore, we established that a CA-NFAT1 C-terminal deletion is sufficient to completely abrogate the proapoptotic function of NFAT1 and that this truncated protein induces a partially transformed phenotype in NIH 3T3 cells resembling the CA-NFAT2-induced phenotype (Fig. 6 and 7). This is the first time that a dual role in the control of the cell cycle and cell death has been characterized within the NFAT family of transcription factors in the same model, although evidence of this dichotomy is progressively emerging.

Recent studies suggest that the NFAT family of transcription factors plays a much broader role in the cell cycle than previously believed, and their contributions to tumorigenesis are becoming clearer. In fact, calcineurin is the major regulator of NFAT activation, and the observation that some human B- and T-cell lymphomas have sustained calcineurin activation suggests that NFAT proteins play a role in tumorigenesis (28). Furthermore, calcineurin activation is essential for tumor progression in a mouse model of lymphoma malignancy (28). Nevertheless, NFAT2 expression has also been linked to several malignant transformations, such as in diffuse large-B-cell and Burkitt's lymphomas (26, 33) and colon and pancreatic carcinomas (14, 18), where it has been demonstrated that NFAT2 expression and activation are essential to the development of cancer. On the other hand, a recent study showed that hypermethylation of the NFAT2 promoter region leads to reduced expression of the protein in human classical Hodgkin's lymphoma and human anaplastic large-cell lymphomas (2). Although these reports seem contradictory to our data, there is evidence that these lymphoma cells have also lost the immu-

noreceptor signaling pathway, suggesting that the need for NFAT signaling in tumorigenesis has been bypassed (4, 40). Furthermore, ectopic expression of the CA-NFAT2 short isoform in the 3T3-L1 preadipocyte cell line established that this was sufficient to induce a transformed phenotype. NFAT2 activation is also implicated in the expression of several cell cycle and survival factors, including cyclins D1 and D2, c-Myc, cyclooxygenase 2, CD40 ligand, and BLyS, that could ultimately aid in tumor growth and apoptosis evasion (5, 15, 20, 30, 33). Furthermore, NFAT2 null mice are embryonic lethal, resulting from a serious malformation of heart valves, while NFAT2$^{-/-}$ × RAG-1$^{-/-}$ chimeric mice showed reduced numbers of thymocytes and impaired proliferation of peripheral lymphocytes, suggesting an important role of the transcription factor in the positive regulation of cell proliferation (13, 35, 36, 45). Our results strongly corroborate these observations and directly demonstrate that sustained activation of NFAT2 short isoform is sufficient to induce cell cycle progression and is able to transform an immortalized cell line. Conversely, it has been previously demonstrated that lymphocytes from NFAT1$^{-/-}$ mice hyperproliferate and that these mice display splenomegaly and delayed thymic involution compared to wild-type mice (39, 44). Ranger et al. also reported that NFAT1$^{-/-}$ mice develop an extraosseous cartilaginous mass resembling a chondrosarcoma (37). Furthermore, NFAT1 was shown to be able to directly bind to the promoter regions and to negatively regulate two cell cycle controllers, CDK4 and cyclin A2, resulting in a substantial reduction of their protein levels, although the relevance of this reduction to the cell cycle and proliferation was not assessed (3, 7). Although the downregulation of these genes could account for the cell cycle arrest in the G_1/S phase that we observed in NIH 3T3 cells expressing CA-NFAT1, the mechanism underlying this phenotype remains unknown. Since the regulation of signaling through each of the pathways mentioned above is known to influence various aspects of the tumorigenic phenotype, it will be interesting to determine if any of these effects are mediated by different actions of NFAT1 and NFAT2.

Other evidently different roles for NFAT family members in the biology of NIH 3T3 cells are in the control of apoptosis. We have demonstrated that NFAT1 and NFAT2 short isoform act in opposition in the control of apoptosis. Apoptosis operates in adult organisms to maintain normal cellular homeostasis; the violation of this cellular process can result in cancer, autoimmunity, and other diseases. NFAT1 and NFAT2 are highly expressed in peripheral T cells, where they are involved in the control of the termination of the immune response by inducing apoptosis. Activation-induced cell death (AICD) is a particular form of apoptosis that is important for the maintenance of immune system homeostasis. One important route of AICD is the activation of so-called death receptors by its ligands, in particular, FasL, tumor necrosis factor alpha (TNF-α), and, more recently, TRAIL. It has been shown that NFAT directly regulates FasL protein expression by binding to its promoter and inducing transactivation (21). Another possible target for NFAT regulation is TRAIL, a novel member of the TNF family of proapoptotic factors. The TRAIL promoter has several putative binding sites for NFAT transcription factors and has been shown to be regulated by NFAT in luciferase reporter assays (22, 43). Although these two mechanisms may be relevant in the activation of cell death, there is no evidence of different roles in their regulation by distinct NFAT family members. An interesting target for NFAT regulation is the TNF-α gene. While NFAT2 proteins are unable to bind and transactivate the TNF-α promoter due to a low affinity of the NFAT2 DBD for the TNF-α promoter, NFAT1 is able to do so, leading to increased expression of TNF-α protein (32). This suggests a possible difference between these two proteins in the control of cell death through TNF-α regulation. Although the activation of the TNF-α gene could explain the ability of CA-NFAT1, but not CA-NFAT2, to induce apoptosis in our model, it does not explain why CA-NFAT1ΔC did not induce apoptosis, as it contains exactly the same DBD as NFAT1 and, presumably, the same affinity for the TNF-α promoter region.

The observation that CA-NFAT1 induces apoptosis and cell cycle arrest while CA-NFAT1ΔC and CA-NFAT2 prevent apoptosis induced by serum withdrawal and lead to increased proliferation of NIH 3T3 cells indicates that these transcription factors (NFAT1 and NFAT2) exhibit both individual and overlapping properties and that the functional differences are partially due to the C terminus of NFAT1. However, we cannot attribute the oncogenic capacity of NFAT2 short isoform totally to the lack of the long C-terminal domain, since the NFAT1ΔC truncated protein is not able to induce tumor formation in BALB/c nude mice (Fig. 7G). The NFAT1 C-terminal domain shows sequence similarity to the corresponding regions of human NFAT2 long isoform, NFAT3, or NFAT4 (38). The C termini of human NFAT1 and NFAT2 long isoforms are capable of transactivation, defining this region as having a transcriptional regulatory role (9, 24). One possibility is that the NFAT transcription factor acts by activating apoptosis and inducing cell cycle arrest through the transactivation of target genes by the conserved C-terminal region of the protein. Until now, there has been only limited evidence that the NFAT C-terminal domain acts as an antioncogene, which is in agreement with our data. Recently, using a model of T-cell lymphoma induction by a T-cell lymphomagenic retrovirus (SL3-3) in mice, it was shown that the C terminus of NFAT4 is a target for retroviral insertion (16). Lymphomas in mice infected with the SL3-3 virus occur when there is an insertion in the promoter region of NFAT4, which blocks protein synthesis, or at the 3′ region of intron 8 of the NFAT4 gene, leading to the generation of an NFAT4 short isoform, which lacks the C-terminal region but still contains a DBD that is similar in length to that of the NFAT2 short isoform. Furthermore, the lack of NFAT4 in mice (NFAT4$^{-/-}$) leads to an increased susceptibility to lymphoma induced by virus infection (16). This suggests that NFAT4 is also a tumor suppressor gene and that the lack of its C terminus is sufficient to inhibit this role. This is also true for the NFAT2 gene, in which several viral insertions at intron 9 were found in different types of cancer models induced by viral insertion (Mouse Retrovirus Tagged Cancer Gene Database [1]). The insertion at intron 9 leads to the formation of the NFAT2 short isoform and prevents the inclusion of the long C terminus that we are proposing to be a tumor suppressor domain of the NFAT transcription factor family. Another interesting correlation that can be made is that murine expression of the NFAT1 short isoform lacking the long C terminus is unique to the brain and heart tissues (34). Since both organs are not capable of self-regeneration and are

continuously subject to calcium influx leading to NFAT activation, these tissues are susceptible to NFAT1-induced apoptosis and, consequently, tissue damage. Although these organs may also have the long-isoform NFATs, one may assume that the overexpression of their smaller counterparts could prevent apoptosis by competing to target proapoptotic promoters.

While it remains to be shown in future studies whether the C termini of NFAT proteins differ in the control of apoptosis and the cell cycle, the study presented here shows a remarkable difference in the phenotypes induced by NFAT1 and NFAT2 proteins. The individual effects induced by NFAT proteins may rely on their capability to control the expression of both pro- and antiapoptotic, as well as cell cycle, genes. This suggests that the cellular threshold levels for each NFAT protein and the protein isoform that is being expressed determine which set of target genes will be expressed and, ultimately, the fate of the cell. In naive peripheral T lymphocytes, NFAT1 and NFAT2 long isoform are the prevalent proteins. T-cell receptor engagement leads to a massive induction of the NFAT2 short isoform, while NFAT1 levels remain constant and the NFAT2 long isoform levels are dramatically reduced (9), suggesting that the induction of the NFAT2 short isoform in T lymphocytes might ensure that these cells exert their effector function without inducing rapid apoptosis. In fact, it has been shown that overexpression of human NFAT1 or NFAT2 long isoform leads to an increase of AICD in primary $CD4^+$ T cells while NFAT2 short-isoform overexpression has no impact on AICD (11). These results give support to our data, which demonstrate that the C-terminal domain of the NFAT1 protein regulates apoptosis (Fig. 6). Moreover, our data also demonstrate that NFAT1 signaling abolishes the effect of NFAT2 short isoform (Fig. 8). However, more studies need to be done in order to better understand the physiological role of the balance between NFAT1 and NFAT2 short isoform. The presence of a domain in the NFAT family members that is capable of inducing an antioncogenic phenotype agrees with the intrinsic tumor suppression mechanism, in which oncogenes can carry their own suppression machinery to avoid cancer development (23). c-Myc is a good example of this property, as it has the ability to induce both tumor formation and apoptosis and its antioncogenic function, which can be suppressed by mutation or alternative splicing, resides at it N terminus (8). NFAT family members might work in the same way and may thus act as tumor suppressors or oncogenes.

ACKNOWLEDGMENTS

We are especially grateful to A. Rao for comments on the work and the manuscript. We are also grateful to A. Rao for kindly providing the NFAT1 plasmids and $NFAT1^{-/-}$ mice, S. Lowe for the pBabe-H-*rasV12* plasmid, and M. Brown for the pcDNA3-NFAT2/A plasmid.

This work was supported by grants from the International Centre for Genetic Engineering and Biotechnology (ICGEB) (CRP/BRA04-02 to J.P.B.V.), the Brazilian National Council for Research (CNPq) (472819/2003-8 and 400968/2005-3 to J.P.B.V.), and the NIH Fogarty International Center (FIRCA) (RO3-TW006466-01 to J.P.B.V.). B.K.R. and A.L.S.C. were supported by a CNPq fellowship and G.P.M. by a CAPES fellowship.

REFERENCES

1. **Akagi, K., T. Suzuki, R. M. Stephens, N. A. Jenkins, and N. G. Copeland.** 2004. RTCGD: retroviral tagged cancer gene database. Nucleic Acids Res. **32:**D523–D527.
2. **Akimzhanov, A., L. Krenacs, T. Schlegel, S. Klein-Hessling, E. Bagdi, E. Stelkovics, E. Kondo, S. Chuvpilo, P. Wilke, A. Avots, S. Gattenlohner, H. K. Muller-Hermelink, A. Palmetshofer, and E. Serfling.** 2008. Epigenetic changes and suppression of the nuclear factor of activated T cell 1 (NFATC1) promoter in human lymphomas with defects in immunoreceptor signaling. Am. J. Pathol. **172:**215–224.
3. **Baksh, S., H. R. Widlund, A. A. Frazer-Abel, J. Du, S. Fosmire, D. E. Fisher, J. A. DeCaprio, J. F. Modiano, and S. J. Burakoff.** 2002. NFATc2-mediated repression of cyclin-dependent kinase 4 expression. Mol. Cell **10:**1071–1081.
4. **Bonzheim, I., E. Geissinger, S. Roth, A. Zettl, A. Marx, A. Rosenwald, H. K. Muller-Hermelink, and T. Rudiger.** 2004. Anaplastic large cell lymphomas lack the expression of T-cell receptor molecules or molecules of proximal T-cell receptor signaling. Blood **104:**3358–3360.
5. **Buchholz, M., A. Schatz, M. Wagner, P. Michl, T. Linhart, G. Adler, T. M. Gress, and V. Ellenrieder.** 2006. Overexpression of c-myc in pancreatic cancer caused by ectopic activation of NFATc1 and the $Ca2^+$/calcineurin signaling pathway. EMBO J. **25:**3714–3724.
6. **Caetano, M. S., A. Vieira-de-Abreu, L. K. Teixeira, M. B. Werneck, M. A. Barcinski, and J. P. Viola.** 2002. NFATC2 transcription factor regulates cell cycle progression during lymphocyte activation: evidence of its involvement in the control of cyclin gene expression. FASEB J. **16:**1940–1942.
7. **Carvalho, L. D., L. K. Teixeira, N. Carrossini, A. T. Caldeira, K. M. Ansel, A. Rao, and J. P. Viola.** 2007. The NFAT1 transcription factor is a repressor of cyclin A2 gene expression. Cell Cycle **6:**1789–1795.
8. **Chang, D. W., G. F. Claassen, S. R. Hann, and M. D. Cole.** 2000. The c-Myc transactivation domain is a direct modulator of apoptotic versus proliferative signals. Mol. Cell. Biol. **20:**4309–4319.
9. **Chuvpilo, S., A. Avots, F. Berberich-Siebelt, J. Glockner, C. Fischer, A. Kerstan, C. Escher, I. Inashkina, F. Hlubek, E. Jankevics, T. Brabletz, and E. Serfling.** 1999. Multiple NF-ATc isoforms with individual transcriptional properties are synthesized in T lymphocytes. J. Immunol. **162:**7294–7301.
10. **Chuvpilo, S., M. Zimmer, A. Kerstan, J. Glockner, A. Avots, C. Escher, C. Fischer, I. Inashkina, E. Jankevics, F. Berberich-Siebelt, E. Schmitt, and E. Serfling.** 1999. Alternative polyadenylation events contribute to the induction of NF-ATc in effector T cells. Immunity **10:**261–269.
11. **Chuvpilo, S., E. Jankevics, D. Tyrsin, A. Akimzhanov, D. Moroz, M. K. Jha, J. Schulze-Luehrmann, B. Santner-Nanan, E. Feoktistova, T. Konig, A. Avots, E. Schmitt, F. Berberich-Siebelt, A. Schimpl, and E. Serfling.** 2002. Autoregulation of NFATc1/A expression facilitates effector T cells to escape from rapid apoptosis. Immunity **16:**881–895.
12. **Clipstone, N. A., and G. R. Crabtree.** 1992. Identification of calcineurin as a key signalling enzyme in T-lymphocyte activation. Nature **357:**695–697.
13. **de la Pompa, J. L., L. A. Timmerman, H. Takimoto, H. Yoshida, A. J. Elia, E. Samper, J. Potter, A. Wakeham, L. Marengere, B. L. Langille, G. R. Crabtree, and T. W. Mak.** 1998. Role of the NF-ATc transcription factor in morphogenesis of cardiac valves and septum. Nature **392:**182–186.
14. **Duque, J., M. Fresno, and M. A. Iniguez.** 2005. Expression and function of the nuclear factor of activated T cells in colon carcinoma cells: involvement in the regulation of cyclooxygenase-2. J. Biol. Chem. **280:**8686–8693.
15. **Fu, L., Y. C. Lin-Lee, L. V. Pham, A. Tamayo, L. Yoshimura, and R. J. Ford.** 2006. Constitutive NF-κB and NFAT activation leads to stimulation of the BLyS survival pathway in aggressive B-cell lymphomas. Blood **107:**4540–4548.
16. **Glud, S. Z., A. B. Sorensen, M. Andrulis, B. Wang, E. Kondo, R. Jessen, L. Krenacs, E. Stelkovics, M. Wabl, E. Serfling, A. Palmetshofer, and F. S. Pedersen.** 2005. A tumor-suppressor function for NFATc3 in T-cell lymphomagenesis by murine leukemia virus. Blood **106:**3546–3552.
17. **Hanahan, D., and R. A. Weinberg.** 2000. The hallmarks of cancer. Cell **100:**57–70.
18. **Heit, J. J., A. A. Apelqvist, X. Gu, M. M. Winslow, J. R. Neilson, G. R. Crabtree, and S. K. Kim.** 2006. Calcineurin/NFAT signalling regulates pancreatic beta-cell growth and function. Nature **443:**345–349.
19. **Hodge, M. R., A. M. Ranger, F. Charles de la Brousse, T. Hoey, M. J. Grusby, and L. H. Glimcher.** 1996. Hyperproliferation and dysregulation of IL-4 expression in NF-ATp-deficient mice. Immunity **4:**397–405.
20. **Iniguez, M. A., S. Martinez-Martinez, C. Punzon, J. M. Redondo, and M. Fresno.** 2000. An essential role of the nuclear factor of activated T cells in the regulation of the expression of the cyclooxygenase-2 gene in human T lymphocytes. J. Biol. Chem. **275:**23627–23635.
21. **Latinis, K. M., L. A. Norian, S. L. Eliason, and G. A. Koretzky.** 1997. Two NFAT transcription factor binding sites participate in the regulation of CD95 (Fas) ligand expression in activated human T cells. J. Biol. Chem. **272:**31427–31434.
22. **Liu, Y., G. L. Borchert, A. Surazynski, C. A. Hu, and J. M. Phang.** 2006. Proline oxidase activates both intrinsic and extrinsic pathways for apoptosis: the role of ROS/superoxides, NFAT and MEK/ERK signaling. Oncogene **25:**5640–5647.
23. **Lowe, S. W., E. Cepero, and G. Evan.** 2004. Intrinsic tumour suppression. Nature **432:**307–315.
24. **Luo, C., E. Burgeon, and A. Rao.** 1996. Mechanisms of transactivation by nuclear factor of activated T cells-1. J. Exp. Med. **184:**141–147.

25. **Macian, F.** 2005. NFAT proteins: key regulators of T-cell development and function. Nat. Rev. Immunol. **5:**472–484.
26. **Marafioti, T., M. Pozzobon, M. L. Hansmann, R. Ventura, S. A. Pileri, H. Roberton, S. Gesk, P. Gaulard, T. F. Barth, M. Q. Du, L. Leoncini, P. Moller, Y. Natkunam, R. Siebert, and D. Y. Mason.** 2005. The NFATc1 transcription factor is widely expressed in white cells and translocates from the cytoplasm to the nucleus in a subset of human lymphomas. Br J. Haematol. **128:**333–342.
27. **Marshall, C. J.** 1991. Tumor suppressor genes. Cell **64:**313–326.
28. **Medyouf, H., H. Alcalde, C. Berthier, M. C. Guillemin, N. R. dos Santos, A. Janin, D. Decaudin, H. de The, and J. Ghysdael.** 2007. Targeting calcineurin activation as a therapeutic strategy for T-cell acute lymphoblastic leukemia. Nat. Med. **13:**736–741.
29. **Monticelli, S., and A. Rao.** 2002. NFAT1 and NFAT2 are positive regulators of IL-4 gene transcription. Eur. J. Immunol. **32:**2971–2978.
30. **Neal, J. W., and N. A. Clipstone.** 2003. A constitutively active NFATc1 mutant induces a transformed phenotype in 3T3-L1 fibroblasts. J. Biol. Chem. **278:**17246–17254.
31. **Okamura, H., J. Aramburu, C. Garcia-Rodriguez, J. P. Viola, A. Raghavan, M. Tahiliani, X. Zhang, J. Qin, P. G. Hogan, and A. Rao.** 2000. Concerted dephosphorylation of the transcription factor NFAT1 induces a conformational switch that regulates transcriptional activity. Mol. Cell **6:**539–550.
32. **Oum, J. H., J. Han, H. Myung, M. Hleb, S. Sharma, and J. Park.** 2002. Molecular mechanism of NFAT family proteins for differential regulation of the IL-2 and TNF-alpha promoters. Mol. Cell **13:**77–84.
33. **Pham, L. V., A. T. Tamayo, L. C. Yoshimura, Y. C. Lin-Lee, and R. J. Ford.** 2005. Constitutive NF-κB and NFAT activation in aggressive B-cell lymphomas synergistically activates the CD154 gene and maintains lymphoma cell survival. Blood **106:**3940–3947.
34. **Plyte, S., M. Boncristiano, E. Fattori, F. Galvagni, S. R. Paccani, M. B. Majolini, S. Oliviero, G. Ciliberto, J. L. Telford, and C. T. Baldari.** 2001. Identification and characterization of a novel nuclear factor of activated T-cells-1 isoform expressed in mouse brain. J. Biol. Chem. **276:**14350–14358.
35. **Ranger, A. M., M. J. Grusby, M. R. Hodge, E. M. Gravallese, F. C. de la Brousse, T. Hoey, C. Mickanin, H. S. Baldwin, and L. H. Glimcher.** 1998. The transcription factor NF-ATc is essential for cardiac valve formation. Nature **392:**186–190.
36. **Ranger, A. M., M. Oukka, J. Rengarajan, and L. H. Glimcher.** 1998. Inhibitory function of two NFAT family members in lymphoid homeostasis and Th2 development. Immunity **9:**627–635.
37. **Ranger, A. M., L. C. Gerstenfeld, J. Wang, T. Kon, H. Bae, E. M. Gravallese, M. J. Glimcher, and L. H. Glimcher.** 2000. The nuclear factor of activated T cells (NFAT) transcription factor NFATp (NFATc2) is a repressor of chondrogenesis. J. Exp. Med. **191:**9–22.
38. **Rao, A., C. Luo, and P. G. Hogan.** 1997. Transcription factors of the NFAT family: regulation and function. Annu. Rev. Immunol. **15:**707–747.
39. **Schuh, K., B. Kneitz, J. Heyer, U. Bommhardt, E. Jankevics, F. Berberich-Siebelt, K. Pfeffer, H. K. Muller-Hermelink, A. Schimpl, and E. Serfling.** 1998. Retarded thymic involution and massive germinal center formation in NF-ATp-deficient mice. Eur. J. Immunol. **28:**2456–2466.
40. **Schwering, I., A. Brauninger, U. Klein, B. Jungnickel, M. Tinguely, V. Diehl, M. L. Hansmann, R. Dalla-Favera, K. Rajewsky, and R. Kuppers.** 2003. Loss of the B-lineage-specific gene expression program in Hodgkin and Reed-Sternberg cells of Hodgkin lymphoma. Blood **101:**1505–1512.
41. **Shibasaki, F., E. R. Price, D. Milan, and F. McKeon.** 1996. Role of kinases and the phosphatase calcineurin in the nuclear shuttling of transcription factor NF-AT4. Nature **382:**370–373.
42. **Viola, J. P., L. D. Carvalho, B. P. Fonseca, and L. K. Teixeira.** 2005. NFAT transcription factors: from cell cycle to tumor development. Braz. J. Med. Biol. Res. **38:**335–344.
43. **Wang, Q., Y. Ji, X. Wang, and B. M. Evers.** 2000. Isolation and molecular characterization of the 5′-upstream region of the human TRAIL gene. Biochem. Biophys. Res. Commun. **276:**466–471.
44. **Xanthoudakis, S., J. P. Viola, K. T. Shaw, C. Luo, J. D. Wallace, P. T. Bozza, D. C. Luk, T. Curran, and A. Rao.** 1996. An enhanced immune response in mice lacking the transcription factor NFAT1. Science **272:**892–895.
45. **Yoshida, H., H. Nishina, H. Takimoto, L. E. Marengere, A. C. Wakeham, D. Bouchard, Y. Y. Kong, T. Ohteki, A. Shahinian, M. Bachmann, P. S. Ohashi, J. M. Penninger, G. R. Crabtree, and T. W. Mak.** 1998. The transcription factor NF-ATc1 regulates lymphocyte proliferation and Th2 cytokine production. Immunity **8:**115–124.